Immunotargeting of the xCT Cystine/Glutamate Antiporter Potentiates the Efficacy of HER2-Targeted Immunotherapies in Breast Cancer

Laura Conti[1], Elisabetta Bolli[1], Antonino Di Lorenzo[1], Valentina Franceschi[2], Francesca Macchi[2], Federica Riccardo[1], Roberto Ruiu[1], Luca Russo[2], Elena Quaglino[1], Gaetano Donofrio[2], and Federica Cavallo[1]

ABSTRACT

Despite HER2-targeted therapies improving the outcome of HER2$^+$ breast cancer, many patients experience resistance and metastatic progression. Cancer stem cells (CSC) play a role in this resistance and progression, thus combining HER2 targeting with CSC inhibition could improve the management of HER2$^+$ breast cancer. The cystine–glutamate antiporter, xCT, is overexpressed in mammary CSCs and is crucial for their redox balance, self-renewal, and resistance to therapies, representing a potential target for breast cancer immunotherapy. We developed a combined immunotherapy targeting HER2 and xCT using the Bovine Herpes virus-4 vector, a safe vaccine that can confer immunogenicity to tumor antigens. Mammary cancer–prone BALB-neuT mice, transgenic for rat *Her2*, were immunized with the single or combined vaccines. Anti-HER2 vaccination slowed primary tumor growth, whereas anti-xCT vaccination primarily prevented metastasis formation. The combination of the two vaccines exerted a complementary effect by mediating the induction of cytotoxic T cells and of HER2 and xCT antibodies that induce antibody-dependent cell-mediated cytotoxicity and hinder cancer cell proliferation. Antibodies targeting xCT, but not those targeting HER2, directly affected CSC viability, self-renewal, and migration, inducing the anti-metastatic effect of xCT vaccination. Our findings present a new therapy for HER2$^+$ breast cancer, demonstrating that CSC immunotargeting via anti-xCT vaccination synergizes with HER2-directed immunotherapy.

Introduction

Breast cancer is one of the three most prevalent cancers worldwide, and the most common in women (1). Breast cancer prognosis has improved because of the progresses achieved in early detection and therapy (2). However, breast cancer is still the second leading cause of cancer-related deaths in developed countries, and its incidence and mortality are progressively increasing in Asia, Africa, and South America (2).

Roughly 20% of breast cancers worldwide overexpress or amplify the *HER2* (erb-b2 receptor tyrosine kinase 2, *ERBB2*) oncogene. Although HER2 positivity associates with poor prognosis and response to standard chemotherapies, the introduction of HER2 mAbs and inhibitors has improved disease-free and overall survival (OS) of patients with HER2$^+$ breast cancer (3). However, most patients affected by metastatic disease display primary or secondary resistance to HER2-targeted therapies, leading to disease progression, with advanced HER2$^+$ breast cancer remaining almost incurable (4). Therefore, the development of new therapeutic approaches that increase the efficacy of HER2-targeting drugs is urgently needed.

Breast cancer stem cells (CSC) are one of the cause for primary resistance to HER2-targeted therapies; their presence is a negative prognostic factor for sensitivity to the HER2 mAb, trastuzumab (5). Therefore, CSC targeting may cooperate with HER2-directed therapies and prevent the development of secondary resistance, resulting in improved patient outcome (6, 7).

xCT, a multipass transmembrane protein encoded by the gene solute carrier family 7 member 11 (*SLC7A11*), is overexpressed in breast CSCs and plays a key role in their self-renewal and resistance to chemotherapy (8). xCT is the light chain of the antiporter system x_c^-, which mediates the cell uptake of cystine in exchange with glutamate (9). Glutamate released in the tumor microenvironment by xCT activates the suppressive function of T regulatory cells (Treg) and promotes breast cancer cell invasion (10, 11), whereas imported cystine is reduced to cysteine, the rate-limiting precursor in the synthesis of glutathione (GSH; ref. 9). GSH is the main intracellular antioxidant molecule that protects cells from ferroptosis, differentiation, autophagy, senescence, and toxicity induced by xenobiotics such as chemotherapeutic drugs (9).

xCT is poorly expressed in healthy tissues but overexpressed in different tumor types, including breast cancer of different histologic subtypes, where its expression is particularly increased in CSCs (8, 9). In breast cancer, xCT is overexpressed in atypical hyperplasia and invasive ductal carcinoma of different histologic subtypes (8) and is linked to poor prognosis in patients with triple-negative breast cancer (TNBC; ref. 12). Therefore, xCT is a promising therapeutic target for breast cancer.

[1]Department of Molecular Biotechnology and Health Sciences, University of Torino, Torino, Italy. [2]Department of Medical Veterinary Sciences, University of Parma, Parma, Italy.

Note: Supplementary data for this article are available at Cancer Immunology Research Online (http://cancerimmunolres.aacrjournals.org/).

G. Donofrio and F. Cavallo contributed equally to this article.

Corresponding Authors: Laura Conti, University of Torino, Via Nizza, 52, Torino 10126, Italy. Phone: 39 011 6706458; Fax: 39 011 2366457; E-mail: laura.conti@unito.it; Federica Cavallo, Phone: 39 011 670 6457; E-mail: federica.cavallo@unito.it; and Gaetano Donofrio, Department of Medical Veterinary Sciences, University of Parma, Strada del Taglio 10, Parma 43126, Italy. Phone: 39 0521 902677; Fax: 39 0521 032672; E-mail: gaetano.donofrio@unipr.it

Cancer Immunol Res 2020;8:1039–53

doi: 10.1158/2326-6066.CIR-20-0082

A variety of compounds have been investigated that pharmacologically inhibit xCT, among them are erastin (13) and the FDA-approved drugs sulfasalazine (14) and sorafenib (13). Erastin and sulfasalazine are insoluble under physiologic conditions, and have poor metabolic stability and pharmacokinetics, precluding their reliable use *in vivo* (9). Sulfasalazine and sorafenib also display low specificity for xCT and inhibit NF-κB and various kinases, respectively, leading to detrimental side effects (9, 13, 15). Therefore, new ways to specifically target xCT need to be developed for clinical use. We previously developed different vaccine platforms to specifically target xCT-expressing breast CSCs. xCT vaccination with the aforementioned approach effectively impairs cancer growth and metastatic dissemination in syngeneic transplantable mouse models of breast cancer (8, 16, 17).

As a proof of concept that xCT vaccination may ameliorate the efficacy of HER2-targeted therapies, we developed a combined immunotherapy administering Bovine Herpes virus-4 (BoHV-4)–based vaccines targeting HER2 (BoHV-4-HER2) and xCT (BoHV-4-xCT) in a preclinical model of $HER2^+$ mammary carcinogenesis (18). BoHV-4 is a promising and safe vaccination strategy that induces a strong immune response to heterologous antigens, breaking the immune tolerance toward cancer-associated antigens (16, 19). BoHV-4-xCT is superior to other anti-xCT vaccines in inducing a specific immune response, as it is the only vector able to break the $CD8^+$ T-cell tolerance and induce xCT-specific cytotoxic T lymphocytes (8, 9, 16, 17). Here, we demonstrated that the combination of HER2- and xCT-targeting synergistically impairs breast cancer progression, with anti-HER2 vaccine inducing an immune response able to hinder the growth of primary tumors, and anti-xCT vaccination impairing CSC survival and metastatic dissemination.

Materials and Methods

Cell and tumorsphere cultures

SKBR3, 4T1, and HEK-293T cells were purchased from ATCC between 2014 and 2018, expanded and aliquoted, and then passaged in our laboratory for fewer than 10 passages after their resuscitation. They were cultured, respectively, in McCoy 5A Modified Medium (SKBR3) or RPMI (Thermo Fisher Scientific) with 10% FBS (Sigma-Aldrich). TUBO cells, derived from a BALB-neuT primary tumor (20), and NIH/3T3 mouse fibroblasts transfected with $H\text{-}2K^d$ and B7.1 (3T3/kB), and with human (3T3/EkB) or rat *Her-2* (3T3/NkB; ref. 21) were cultured in DMEM (Thermo Fisher Scientific) with 20% FBS. Cells were tested negative for *Mycoplasma* (22) and not authenticated in the past year. Tumorspheres were generated as in (23) and cultured in serum-free DMEM-F12 Medium (Thermo Fisher Scientific) supplemented with 20 ng/mL basic FGF, 20 ng/mL EGF, 5 μg/mL insulin, and 0.4% BSA (all from Sigma-Aldrich). This medium will be referred to as "tumorsphere medium."

Vaccine generation and *in vivo* treatment

BoHV-4-HER2 (*alias* BoHV-4-RHuT-gD), BoHV-4-xCT, and the control vector BoHV-4-ctrl (*alias* BoHV-4-A29) were generated and $TCID_{50}$ quantified as described previously (16, 19). Female BALB-neuT mice were generated and maintained at Molecular Biotechnology Center, University of Torino (Torino, Italy). The animal studies were conducted in accordance with European guidelines, Directive 2010/63, and with the approval of the Animal Care and Use Committee of University of Torino (Torino, Italy) and of the Italian Ministry of Health (authorizations N° 237/2015-PR and 500/2017-PR). Mice were vaccinated six times by intraperitoneal injections of 100 μL of DMEM containing 10^6 $TCID_{50}$ of BoHV-4-ctrl, BoHV-4-xCT, and/or BoHV-4-HER2 at 2-week intervals, starting from 6 weeks of age; immune sera were collected by retro-orbital bleeding at weeks 14 and 18. Mice were inspected weekly with a caliper, and progressively growing masses with mean diameter >1 mm were considered tumors. Growth was monitored until all 10 mammary glands displayed a tumor or a tumor exceeded 10 mm mean diameter, then mice were culled, and blood, spleen, lungs, and tumors collected and processed as described below. Superficial lung metastases were counted with Zeiss SEMI DV4 Spot stereomicroscope.

RNA extraction and real-time PCR

Autochthonous mammary tumors were resected from female BALB-neuT mice immediately after euthanasia and incubated overnight at 4°C in RNAlater Stabilization Solution (Thermo Fisher Scientific). Tumor samples were subsequently removed from RNAlater stabilization solution and stored at −80°C until use. Total RNA was isolated from thawed tumor tissues homogenized through an Ultra-Turrax Disperser (IKA) using the TRizol Reagent (Thermo Fisher Scientific, catalog no. 15596-026), following the manufacturer's instructions.

Genomic DNA contaminations were removed from 10 μL of RNA samples with the Ambion DNA-Free Kit (Thermo Fisher Scientific, catalog no. AM1906). RNA concentration and quality were assessed with NanoDrop 2000 Spectrophotometer (Thermo Fisher Scientific) and 2100 Bioanalyzer (Agilent Technologies), respectively.

cDNA was obtained from 1 μg of RNA retrotranscribed with Ambion RETROscript Reagents (Thermo Fisher Scientific). Following retrotranscription, resulting cDNA was diluted 1:4 in nuclease-free water, and 5 μL of diluted cDNA was included in a total volume of 20 μL of PCR reaction. Target cDNA was amplified through real-time PCR using either murine *Slc7a11*- or *Gapdh*-specific primers (QuantiTect Primer Assay; Qiagen) and SYBR Green PCR Master Mix (Thermo Fisher Scientific). A 7300 Real-Time PCR System (Thermo Fisher Scientific) was used to perform the real-time PCR and the Applied Biosystems SDS Software Version 1.3.1 (Thermo Fisher Scientific) was used to analyze the data. Two independent biological replicates were included in the experiment, and three technical replicates per sample were probed. Average *Slc7a11* mRNA expression (outputted as threshold cycle – C_t) was normalized on average *Gapdh* mRNA expression levels of the same sample using the ΔC_t method (*Slc7a11* C_t – *Gapdh* C_t). Data were represented as $-\Delta C_t$ for best visualization.

Analysis of vaccination-induced virus-neutralizing antibodies

A total of 0.6×10^5 HEK-293T cells/well were cultured overnight in 48-well plates in DMEM supplemented with 10% FBS. The day after, 1.2×10^5 $TCID_{50}$ of a recombinant BoHV-4 expressing enhanced GFP (BoHV-4-GFP; ref. 24), corresponding to a multiplicity of infection of 2 $TCID_{50}$ per cell, were incubated for 90 minutes at room temperature in 100 μL of DMEM containing or not different dilutions (1:5; 1:10; and 1:20) of pooled sera collected from BALB-neuT mice left untreated or vaccinated six times with BoHV-4–based vectors expressing HER2 and xCT. HEK-293T cells were incubated with the mixture of virus and sera for 3 hours at 37°C, and then in DMEM supplemented with 10% FBS. Twenty-four hours later, the cells were imaged with a 20× objective on a Zeiss Axio Observer inverted microscope, and then collected and analyzed by flow cytometry for GFP expression.

FACS

Tumorsphere-derived cells were incubated with immune sera for 5 days, then dissociated and stained with anti-Sca1-AlexaFluor647,

anti-CD44-PE, and anti-mouse CD24-PE/Cy7 or anti-human CD24-FITC (BioLegend). Intracellular reactive oxygen species (ROS) were stained with 2′,7′-dihydrochlorofluorescein diacetate (Sigma-Aldrich, cod. 35848; ref. 8). Apoptosis was evaluated with Annexin V-Apoptosis Kit-APC (eBioscience, cod. 88-8007-72) following the manufacturer's instructions (25). To evaluate xCT, cells were fixed/permeabilized with BD Cytofix/Cytoperm Kit and stained with anti-xCT rabbit antibody (PA1-16775, Thermo Fisher Scientific) followed by FITC-anti-rabbit-Ig (Dako). Tregs in heparinized blood, collected by retro-orbital bleeding, were stained with anti-mouse-CD45-VioGreen (Miltenyi Biotec), CD4-PE/Cy7, GITR-PE, and CD25-APC (BioLegend), and anti-FoxP3-FITC (eBioscience) as in (26). Fresh primary tumor specimens of 8 to 10 mm mean diameter and lungs were finely minced with blades and digested by incubation with 1 mg/mL collagenase IV (Sigma-Aldrich) in RPMI1640 at 37°C for 1 hour in an orbital shaker. After washing in RPMI1640 with 10% FBS, the cell suspension was passed through a 70-μm pore cell strainer, centrifuged at 1400 rpm for 10 minutes, and incubated in erythrocyte lysing buffer (155 mmol/L NH_4Cl, 15.8 mmol/L Na_2CO_3, and 1 mmol/L EDTA, pH 7.3) for 10 minutes at room temperature. After washing in RPMI1640 with 10% FBS, 1×10^6 cells were collected, resuspended in PBS, treated with Fc-receptor blocker (anti-CD16/CD32 antibody, BD Biosciences; ref. 27), and stained with anti-mouse CD45-VioGreen, CD3-FITC, CD4-APC/Vio770, CD8-VioBlue, PD-1-APC, CD49b-PE (Miltenyi Biotec), CD69-PE/Cy7, CD44-PE, CD24-PE/Cy7, and Sca1-AlexaFluor647 (16). Samples were acquired on BD-FACSVerse and cell populations [natural killer (NK) cells: $CD3^-$ $CD49b^+$; natural killer T cells (NKT): $CD3^+$ $CD49b^+$; $CD4^+$ T cells: $CD3^+$ $CD49b^-$ $CD4^+$; $CD8^+$ T cells: $CD3^+$ $CD49b^-$ $CD8^+$; and Tregs: $CD3^+$ $CD4^+$ $CD25^{high}$ $GITR^+$ $Foxp3^+$] were analyzed with FlowJO10.5.3. tSNE analysis of immune infiltrates was run on five samples per group. FCS3 files were downsampled to 5,000 live $CD45^+$ cells. All the down-samples were then concatenated together into one FCS3 file with the "export concatenated populations" option, and tSNE was run (perplexity, 30; iterations, 1,000). Then dot plots were generated according to experimental groups.

3T3/kB, 3T3/EkB, and 3T3/NkB were incubated with a 1:50 dilution of pooled or single mouse sera for 30 minutes at 4°C, followed by FITC-conjugated rabbit anti-mouse Ig (Dako), then analyzed by FACS. HER2 expression on TUBO, 4T1, and SKBR3 was assessed by staining with the HER2 mAbs Ab4, Ab3, and Ab5 (Merck), respectively, followed by FITC-conjugated rabbit anti-mouse Ig (Dako). All samples were acquired on a BD FACSVerse (BD Biosciences) and analyzed with FlowJO10.5.3.

ELISA

Blood was collected by retro-orbital bleeding of the vaccinated BALB-neuT mice (at 14 and 18 weeks of age) and let to coagulate for 30 minutes at room temperature. Coagulated blood was then centrifuged at 3000 rpm for 10 minutes, and sera (hereafter referred to as immune sera) were collected and stored at −20°C. Thawed sera (1:50) were incubated on plates coated with either recombinant mouse xCT (Cloud-Clone-Corp., 40 ng/well), extracellular rat or human HER2 (Sino Biological, 100 ng/well) proteins, or mouse xCT extracellular loop peptides (GenScript, 1 μg/well), and binding was detected with horseradish peroxidase–conjugated anti-mouse-IgG using a 680XR Microplate Reader (Bio-Rad; refs. 16, 19).

Cytotoxicity

Splenocytes from vaccinated mice were collected by smashing spleens from vaccinated mice on a 40-μm pore cell strainer, centrifuging the resulting cells at 1400 rpm for 10 minutes, and incubating them in erythrocyte lysing buffer for 10 minutes at room temperature. After washing in RPMI1640 with 10% FBS, 20×10^6 splenocytes were resuspended in FBS supplemented with 10% DMSO (Sigma-Aldrich) and stored at −80°C. A total of 1×10^4 4T1 or TUBO target cells were incubated with 2 μmol/L CFSE (Molecular Probes, cod. C34554) for 20 minutes at 37°C, washed with RPMI1640 supplemented with 10% FBS, and then cultured with thawed splenocytes at different effector:target (E:T) ratios for 48 hours. Cells were then stained with 1 μg/mL 7-Amino-ActinomycinD (7-AAD, BD Biosciences), acquired using a BD FACSVerse (BD Biosciences) and analyzed using FlowJO10.5.3 (16). Percent killing was obtained by back-gating on the $CFSE^+$ targets and measuring the percentage of $7\text{-}AAD^+$ dead cells. Percent-specific lysis was calculated with the formula [(dead targets in sample (%) – spontaneously dead targets (%))/(dead target maximum − spontaneously dead targets (%))] × 100. Spontaneous death was obtained by culturing target cells without splenocytes, whereas maximal death was obtained after treatment with PBS supplemented with 1% saponin. For antibody-dependent cell-mediated cytotoxicity (ADCC), E:T incubation was performed overnight in the presence of a 1:50 dilution of immune sera, collected as described in the ELISA section (16).

Immune sera effect on tumorspheres

TUBO and SKBR3 tumorspheres were dissociated and cultured for 5 days in tumorsphere medium supplemented with a 1:50 dilution of immune sera. Contrast phase images were acquired (10×) on a Zeiss Axio Observer or a Leica DMi1 Inverted Microscope connected with a DC120 digital camera. Spheres were then aliquoted in 96-well plates (20 μL/well) and the number of spheres was manually counted under Leica DMi1 Inverted Microscope (4× magnification). Spheres were then collected, dissociated by pipetting several times in trypsin-EDTA, and then the single-cell suspension was processed for FACS analysis of apoptosis, CSC markers, or ROS content (as described in the FACS section). To measure ferroptosis, aliquot of cells dissociated from tumorspheres were cultured for additional 24 hours at 37°C in tumorsphere medium with or without the addition of the iron chelator deferoxamine-mesylate (DFO; 50 μmol/L, Sigma-Aldrich). Cells were then collected and stained with the Annexin V-APC kit (as described in the FACS section) and analyzed by FACS.

Analysis of antibody specificity

Immune sera were incubated for 2 hours at 37°C on plates coated with recombinant xCT, rat or human HER2, or angiomotin (AMOT; Sino Biological, 100 ng/well) protein as a control. Sera were then collected from plates, and aliquots of sera preadsorbed on HER2 were incubated on xCT-coated plates, to deplete both HER2 and xCT antibodies. Unprocessed or preadsorbed sera (1:50) were incubated with TUBO or SKBR3 cells for 30 minutes at 4°C, followed by FITC-conjugated anti-mouse-Ig (Dako) for FACS analysis. TUBO-derived tumorspheres were dissociated as described in the previous paragraph and cultured in tumorsphere medium with the addition of preadsorbed sera (1:50) for 5 days, then tumorspheres were counted.

Cell migration

TUBO and SKBR3 cells were incubated for 1 hour at 37°C in 100 μL of serum-free medium with immune sera (1:20), and then seeded (1×10^5 and 5×10^4, respectively) in the top chamber of 24-Transwell plates (8-μm pores; Corning). Medium with 10% FBS was inserted in bottom chambers, and cells were incubated at 37°C for 48 hours. Cells on the filter top side were detached with cotton-tipped swabs. Cells

migrated to the bottom side were fixed with 2.5% glutaraldehyde and stained with 0.2% crystal violet (Sigma-Aldrich). Four images per well were captured with an Olympus BX41 Microscope, and cells were counted using Fiji software.

MTT

A total of 1×10^4 cells were cultured overnight in 96-well plates. Sera (1:50) were then added, and cells were incubated for 24, 48, or 72 hours. MTT (0.5 mg/mL; Sigma-Aldrich, cod. M2128) was added for 4 hours at 37°C, then supernatants removed and DMSO was added. Absorbance was measured on a 680XR Microplate Reader (Bio-Rad) at 570 and 650 nm (background subtraction).

Meta-analysis on patient databases

Prognostic value of *SLC7a11* mRNA expression in OS, relapse-free survival (RFS), and distant metastasis–free survival (DMFS) of patients with $HER2^+$ breast cancer was analyzed using the open access online software Kaplan–Meier (KM) plotter (https://kmplot.com/analysis/). The background database used by KM plotter is manually curated and contains gene expression data and survival information downloaded from Gene Expression Omnibus, European Genome-phenome Archive, and The Cancer Genome Atlas. Exhaustive information regarding software and datasets is reported in (28). Briefly, the database was queried for *SLC7A11* mRNA expression (Affymetrix ID 209921_at). Patients were stratified in two groups according to high or low *SLC7A11* expression. To define a cutoff between low and high *SLC7A11* expression, all the possible cutoff values between the lower and upper quartiles were computed, and the best performing threshold was used as a cutoff through "auto select best cutoff" function. Analysis was restricted to patients with breast cancer with positive HER2 status ($N = 129$ for OS, $N = 252$ for RFS, and $N = 126$ for DMFS). Removal of redundant samples, exclusion of biased arrays, and proportional hazard assumptions check were included in the quality control. Differences in the OS, DFS, and DMFS for patients with $HER2^+$ breast cancer according to high or low *SLC7A11* mRNA expression were tested for significance using log-rank tests. The output of the analysis included a KM plot representing the survival curves, HR and 95% confidence intervals, numbers at risk, as well as log-rank *P*. Log-rank $P < 0.05$ was considered to be statistically significant.

Statistical analysis

Statistical significance was evaluated using GraphPad8 software. Differences in tumor-free mice were analyzed with Mantel–Cox log-rank test. Two-tailed unpaired Student *t* test was used to assess statistical significance among the groups in sphere formation, tumor multiplicity, cell migration, and the results from FACS and ELISA experiments. Differences in metastasis prevalence and number were analyzed with Fisher exact test and nonparametric Mann–Whitney *U* test, respectively. A threshold of $P < 0.05$ was used to consider significance.

Results

xCT expression was linked to poor prognosis in patients with $HER2^+$ breast cancer

High xCT expression is linked to poor prognosis in patients with TNBC (12). To analyze whether the same was true for $HER2^+$ breast cancer, we ran a meta-analysis on public microarray data (http://kmplot.com/analysis/; ref. 28). Patients with high expression of xCT displayed a significantly lower OS and RFS as compared with patients displaying low xCT (**Fig. 1A** and **B**), and a trend of less DMFS (**Fig. 1C**). This suggested that xCT contributes to $HER2^+$ breast cancer progression, relapse, and metastatic spreading, prompting us to test whether its targeting may improve anti-HER2 immunotherapy.

xCT vaccination potentiated anti-HER2 immunotherapy

The BoHV-4-xCT vaccine, coding for mouse xCT (NP_036120.1), impairs breast CSCs and protects mice from metastases in transplantable mammary cancer models (16). To test whether BoHV-4-xCT improved the outcome of HER2-targeted immunotherapies, we used BALB-neuT mice, whose rat $HER2^+$ mammary tumors express xCT (**Fig. 1D**). BoHV-4-HER2, coding for a chimeric rat/human HER2, was used as HER2-targeting immunotherapy, because it can break BALB-neuT tolerance to rat HER2 (19). Female BALB-neuT mice were immunized by intraperitoneal injections of 10^6 $TCID_{50}$ of BoHV-4-xCT, BoHV-4-HER2, and control BoHV-4-ctrl vectors, alone or in combination. All mice received six immunizations (one every 2 weeks). Each vaccine was administered four times (**Fig. 1E**). xCT expression was higher in 6-week-old BALB-neuT mammary glands than in overt tumors (Supplementary Fig. S1). xCT is important, both in the synthesis of GSH, necessary for cancer initiation but dispensable for its growth (29), and in the maintenance of CSCs, involved in tumor onset (6). Therefore, xCT vaccination was started in the early stages of tumor development (week 6), and HER2 vaccination at week 10 as in (19).

Repeated vaccinations with BoHV-4–based vectors did not induce virus-neutralizing antibodies, as incubation with sera from BoHV-4–vaccinated mice did not impair the infection ability of a GFP-expressing BoHV-4 vector (Supplementary Fig. S2).

All vaccinated mice showed a significantly longer tumor-free survival (**Fig. 1F**) and a slower increase in tumor multiplicity than control mice (**Fig. 1G**). This was more pronounced in mice vaccinated with HER2, alone or combined with xCT. Of note, xCT vaccination protected BALB-neuT mice from the development of lung metastases (**Fig. 1H**). All control and HER2-vaccinated mice displayed lung metastases, but only 54.5% and 63.6% of mice vaccinated with HER2 + xCT or xCT alone ($P = 0.035$ and $P = 0.09$; Fisher exact test), respectively, developed metastases (**Fig. 1H**). The number of lung metastases was significantly reduced by anti-xCT vaccination, alone or combined with HER2 (**Fig. 1I**). Thus, xCT vaccination potentiated the effectiveness of anti-HER2 immunization by significantly hindering the development of metastases.

xCT vaccination decreased CSC frequency in tumors and metastasis-containing lungs

Because CSCs contribute to metastatic dissemination (6), we assessed the frequency of $Sca1^+$ and $CD44^+$ $CD24^-$ CSCs in tumors and lungs from immunized mice. $Sca1^+$ CSCs were detected in both tumors and lungs of control mice (**Fig. 2A** and **B**). Their frequency was significantly reduced by xCT vaccination, alone or combined with HER2, but not by anti-HER2 vaccination (**Fig. 2A** and **B**). A lower percentage of $CD44^+$ $CD24^-$ CSCs, endowed with mesenchymal-like properties (30), was observed in tumors of control and vaccinated mice as compared with lungs (**Fig. 2C** and **D**). Vaccination did not modulate these cells in tumors (**Fig. 2C**), but significantly decreased them in lungs (**Fig. 2D**). These results confirmed that xCT vaccination decreases CSC frequency and suggested a different sensitivity of various CSC populations to HER2 targeting.

HER2 and xCT combined vaccination activated tumor-infiltrating T lymphocytes

Immune cell infiltrates in tumors and lungs of vaccinated mice were analyzed. None of the vaccines significantly increased the

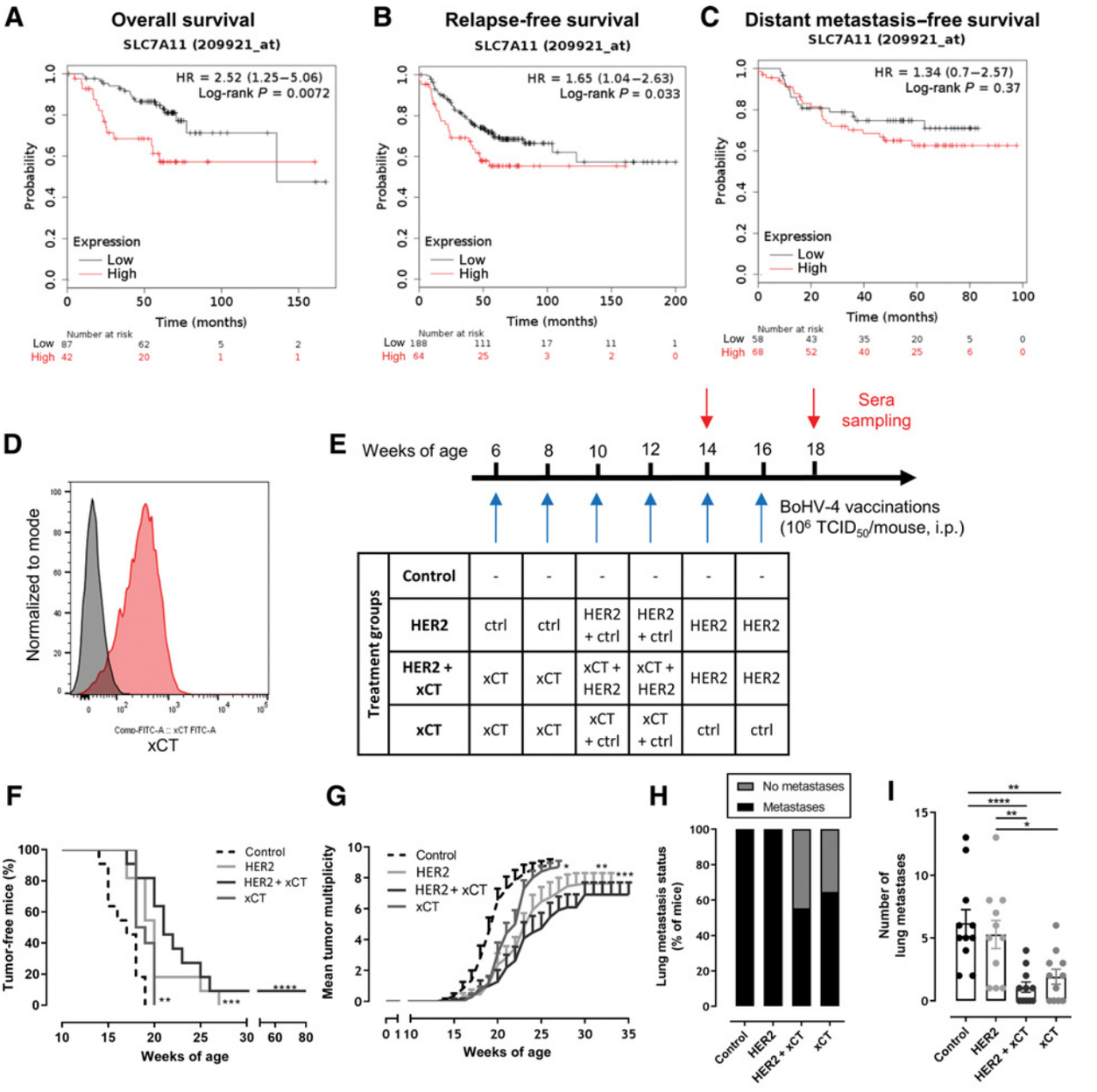

Figure 1.

xCT correlated with poor prognosis in patients with HER2$^+$ breast cancer, and its immunotargeting potentiated anti-HER2 vaccination in BALB-neuT mice. KM plots displaying OS ($N = 129$; **A**), RFS ($N = 252$; **B**), and DMFS ($N = 126$; **C**) in patients with HER2$^+$ breast cancer stratified according to xCT mRNA expression. **D,** Representative ($N = 6$) FACS of xCT (red) or control antibody (gray) on a BALB-neuT mammary tumor. **E–I,** BALB-neuT mice were vaccinated or not (control, ctrl) with BoHV-4-ctrl and BoHV-4-HER2 (HER2); BoHV-4-xCT and BoHV-4-HER2 (HER2 + xCT); and BoHV-4-xCT and BoHV-4-ctrl (xCT; $N = 11$ per group; **E**). Tumor-free survival (**F**) and tumor multiplicity (**G**). **H,** Relative percentage of mice that developed (black) or not (gray) lung metastases. **I,** Mean ± SEM of the number of superficial lung metastases. Each dot represents a mouse. *, $P < 0.05$; **, $P < 0.01$; ***, $P < 0.001$; ****, $P < 0.0001$ compared with controls. Log-rank Mantel–Cox test (**A–C** and **F**), Student t test (**G**), or Mann–Whitney U test (**I**). i.p., intraperitoneal.

percentages of tumor-infiltrating NK, NKT, and CD4$^+$ T lymphocytes as compared with controls (**Fig. 3A** and **B**). However, all vaccines, and particularly HER2 + xCT combination, significantly increased tumor-infiltrating CD8$^+$ T cells (**Fig. 3A** and **B**, orange and red in tSNE plots). As shown in **Fig. 3A** and **C**, all the vaccines induced T-cell activation in tumors, as suggested by the significant increase in CD69$^+$ cells among both CD4$^+$ (yellow) and CD8$^+$ (red) CD3$^+$ T cells, and the combination of HER2 and xCT vaccination significantly increased T-cell activation as compared with anti-HER2 vaccine alone. Anti-xCT vaccination induced

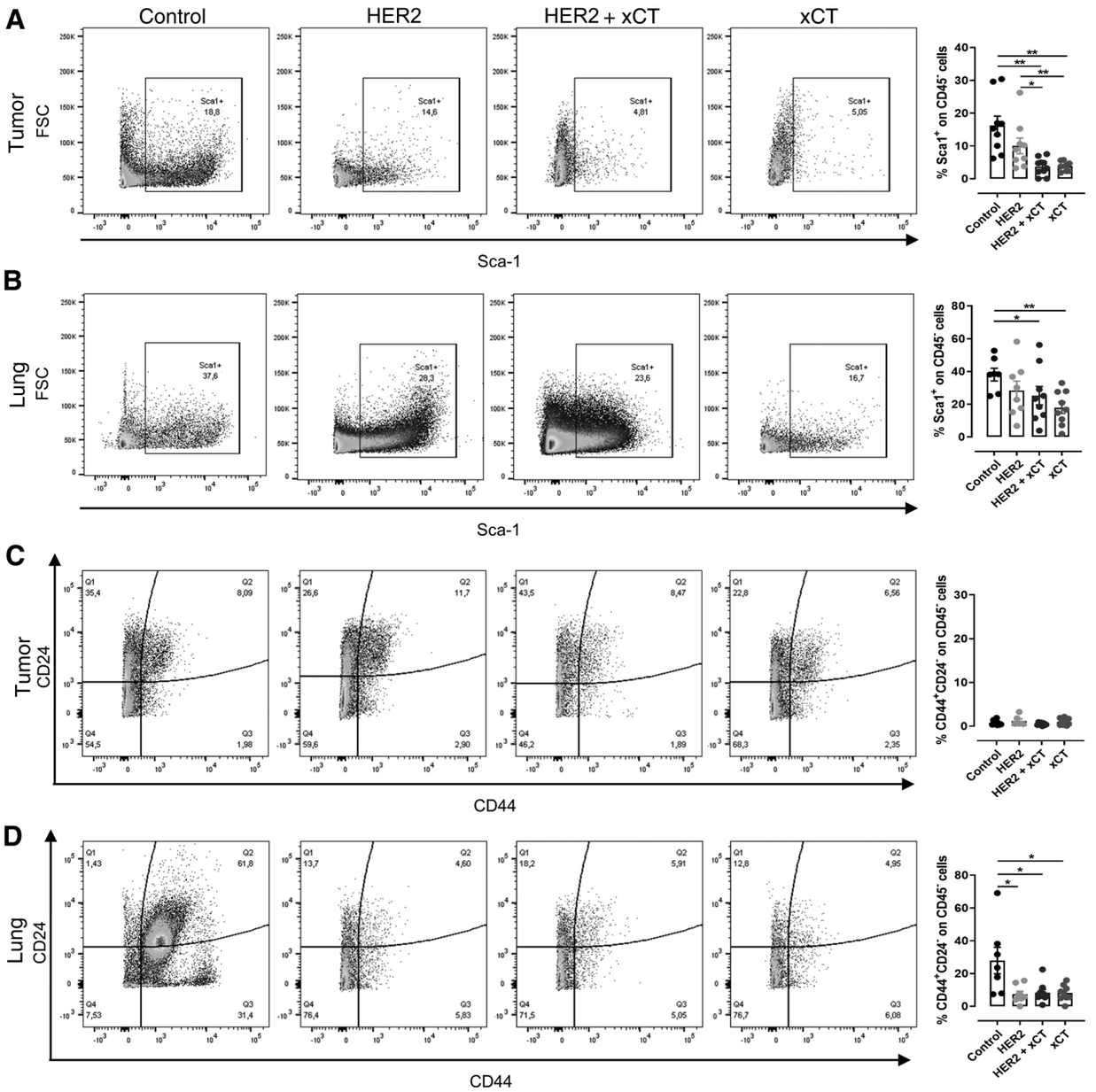

Figure 2.

xCT vaccination decreased CSC frequency in tumors and lungs. Representative ($N \geq 6$ mice per group) FACS of Sca1$^+$ (**A** and **B**) and CD44$^+$ CD24$^-$ CSCs (**C** and **D**) in tumors (**A** and **C**) and lungs (**B** and **D**) from control or vaccinated mice. Graphs show mean ± SEM of the percentage of CSCs among CD45$^-$ cells (each dot represents a mouse). *, $P < 0.05$; **, $P < 0.01$, Student t test.

the activation of NK cells (**Fig. 3A** and **C**, light blue). However, PD-1 expression in NK and T cells was not significantly altered by any vaccines, although a trending decrease of PD1$^+$ CD4$^+$ T cells was observed in mice vaccinated with HER2 + xCT or xCT (**Fig. 3A** and **D**).

None of the vaccines altered the frequency of NK, NKT, or CD4$^+$ T cells in lungs, whereas the combination of HER2 and xCT vaccination significantly increased CD8$^+$ T lymphocytes (**Fig. 3E** and **F**). All vaccinations induced the activation of NK, total CD3$^+$ T, and CD4$^+$ T cells, whereas CD8$^+$ T cells were activated only by anti-xCT vaccination, alone or combined with HER2 (**Fig. 3E** and **G**). As for primary tumors, the treatments did not induce significant variations in the amount of PD-1$^+$ NK or T cells (**Fig. 3E** and **H**).

These data indicated that all the vaccines activated NK and CD4$^+$ T cells in primary tumors and lungs, and CD8$^+$ T lymphocytes in the tumors. However, only xCT vaccination increased the frequency and the activation of CD8$^+$ T lymphocytes in the lungs, possibly explaining its antimetastatic activity.

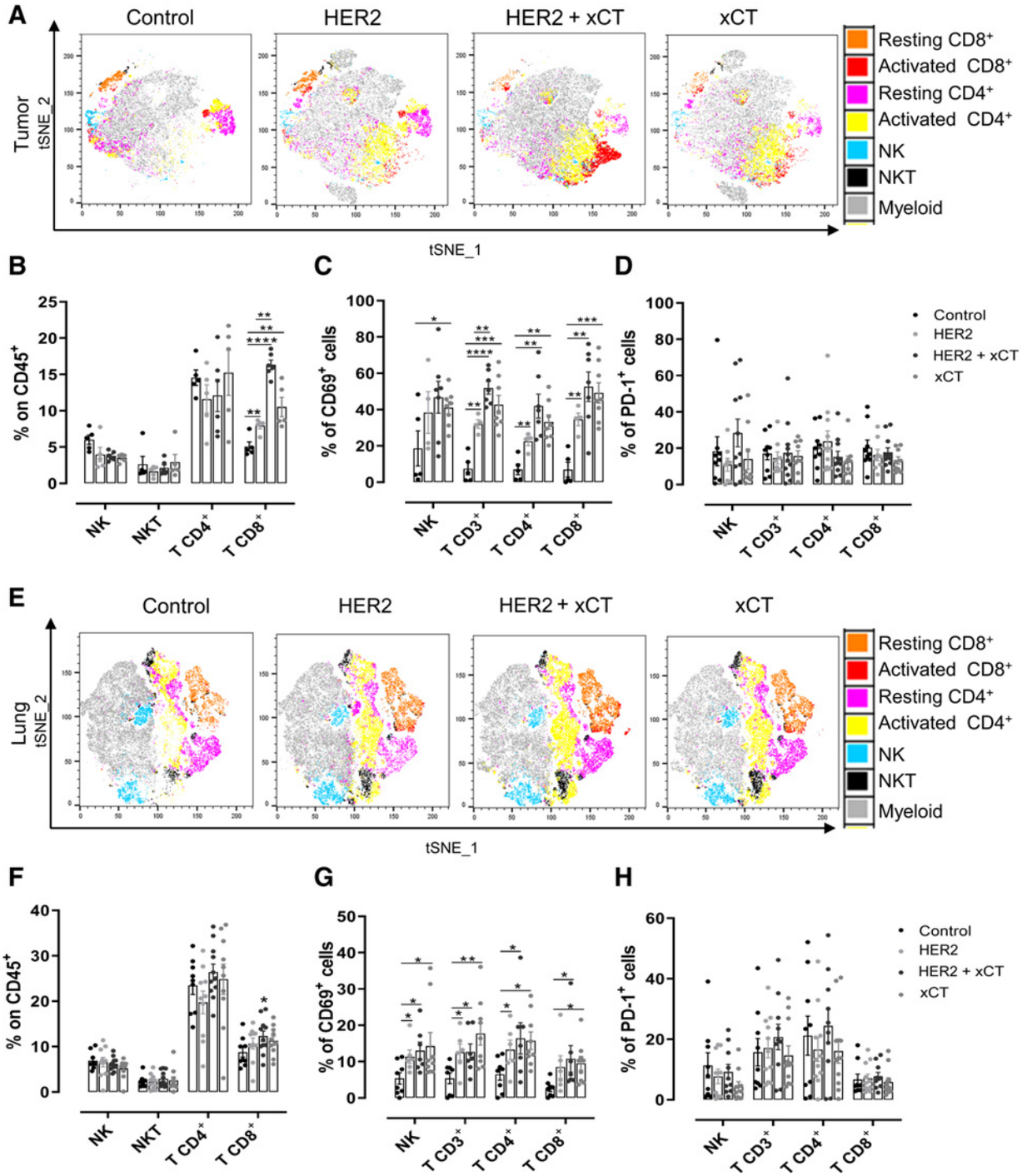

Figure 3.

HER2 and xCT vaccination activated T lymphocytes in tumors and lungs. FACS of immune infiltrates in tumors (**A–D**) and lungs (**E–H**) of control or vaccinated mice. **A** and **E,** tSNE maps show concatenated files for each group of mice (5,000 live CD45$^+$ cells per sample; $N = 5$ per group), with the overlay of manually gated populations. **B** and **F,** Percentage ± SEM of NK, NKT, CD4$^+$, and CD8$^+$ T cells on CD45$^+$ cells. Percentage ± SEM of CD69$^+$ (**C** and **G**) and PD1$^+$ cells (**D** and **H**) among T and NK cells. Each dot represents a mouse. $N \geq 5$ per group. *, $P < 0.05$; **, $P < 0.01$; ***, $P < 0.001$; ****, $P < 0.0001$, Student t test versus control where not otherwise indicated by lines.

Anti-xCT vaccination induced breast cancer cell cytotoxicity and decreased Tregs

To assess whether vaccination-generated T lymphocytes were able to kill $HER2^+$ and/or xCT^+ breast cancer cells, we analyzed *in vitro* cytotoxicity. Splenocytes from vaccinated mice were incubated with rat $HER2^+$ TUBO or TNBC 4T1 cells at different E:T ratios. Both TUBO and 4T1 cells express xCT, whereas only TUBO express HER2 (Supplementary Fig. S3). Because BALB-neuT mice lack high avidity HER2-specific $CD8^+$ T cells due to central tolerance (31), splenocytes from HER2-vaccinated mice did not induce a significant cytotoxicity on TUBO and, as expected, on control 4T1 cells (**Fig. 4A**; Supplementary Fig. S4). On the contrary, anti-xCT vaccination induced a significant cytotoxicity of both cell lines (**Fig. 4A**; Supplementary Fig. S4). This effect was maintained when anti-xCT was combined with anti-HER2 vaccination (**Fig. 4A**; Supplementary Fig. S4), which was accompanied by a reduction of circulating Tregs as compared with control mice (**Fig. 4B**).

HER2 and xCT vaccination induced a specific antibody response that mediates ADCC

HER2- and xCT-specific antibodies were evaluated in the sera of mice 2 weeks after the last vaccination (18-week-old mice). Anti-xCT immunization induced xCT antibodies that were barely detectable in sera from control and HER2-vaccinated mice (**Fig. 5A**). These antibodies bound xCT extracellular loops (**Fig. 5B–F**), suggesting they can play a therapeutic role by binding xCT^+ cancer cells. No differences were observed between mice vaccinated with xCT alone or combined with HER2 (**Fig. 5A–F**). HER2 vaccination–induced antibodies were able to bind both rat and human HER2 (**Fig. 5G** and **H**). Anti-rat and human HER2 antibodies (**Fig. 5G** and **H**) were abundant in sera from xCT-vaccinated mice, suggesting that xCT vaccination may induce cell death and epitope spreading due to the release of HER2 from dead cells. Sera from 14-week-old mice gave similar results (Supplementary Fig. S5A).

The ability of vaccination-induced antibodies to recognize HER2 and xCT on mouse or human tumor cells was assessed, as mouse and human xCT displayed 89% homology. $HER2^+$ xCT^+ TUBO and human SKBR3 breast cancer cells were stained with immune sera and analyzed by FACS. Sera from control mice did not bind TUBO or SKBR3 cells, which were stained by sera from all vaccinated mice (**Fig. 5I–L**; Supplementary Fig. S5B). Binding was higher on SKBR3, which expresses more xCT and HER2 than TUBO (Supplementary Fig. S3). To verify the specificity of sera binding, antigen-specific antibodies were depleted by incubating immune sera with HER2 or xCT recombinant proteins, alone or combined, or with the unrelated AMOT control protein. Preadsorption of immune sera on either HER2 or xCT proteins decreased sera binding to cells, which was further decreased by depletion of both xCT and HER2 antibodies, confirming that vaccination induces antibodies that specifically bind $HER2^+$ xCT^+ tumor cells (**Fig. 5I** and **J**; Supplementary Fig. S5B). As expected, preadsorption on AMOT did not alter sera binding to cells (**Fig. 5I** and **J**; Supplementary Fig. S5B). The specificity of vaccination-induced HER2 antibodies was further confirmed by their ability to stain 3T3 mouse fibroblasts transfected with rat (3T3/NkB cells) or human (3T3/EkB cells) *HER2*, but not untransfected $HER2^-$ xCT^- 3T3/kB cells (Supplementary Fig. S5C).

While the few xCT antibodies present in control mice sera were mainly IgG1, vaccination induced the expansion of specific IgG2a (**Fig. 5K**). Similarly, the proportion of anti-HER2 IgG2a was increased by anti-HER2 vaccination as compared with control mice, with a concomitant reduction of the percentage of IgM and IgG3 (**Fig. 5L**). As IgG2a are the main mediators of ADCC in mice, sera from xCT-vaccinated mice induced ADCC by splenocytes from syngeneic mice of both TUBO and 4T1 cells, whereas sera from HER2-immunized mice only of TUBO cells, as expected. The combination of HER2 and xCT vaccination killed most of the TUBO cells (**Fig. 5M** and **N**).

Her2 and xCT antibodies differentially impaired cancer cell viability and migration

We evaluated the direct effect that immune sera from vaccinated mice exerted on mammary cancer cells. TUBO and SKBR3 cell viability was decreased after 48 and 72 hours of incubation with sera from all vaccinated mice, as compared with sera from control mice (**Fig. 6A** and **B**). This direct impairment of cancer cell viability may contribute to the therapeutic effects *in vivo*.

Because metastatic spreading was decreased in mice vaccinated with xCT, the ability of vaccine-induced antibodies to inhibit cancer cell migration was assessed by transwell assays. As shown in **Fig. 6C**, sera from xCT or HER2 + xCT immunized mice significantly impaired the migration of both TUBO and SKBR3 cells, as confirmed by the decreased number of migrating cells (**Fig. 6D** and **F**) and area covered by migrated cells (**Fig. 6E** and **G**). No effect was exerted by sera of mice vaccinated with HER2 alone (**Fig. 6C–G**), indicating that xCT and Her2 vaccinations have different mechanisms to hamper breast cancer progression, thus supporting the antimetastatic role exerted by xCT vaccination *in vivo*.

Vaccine-induced xCT-targeting antibodies halted CSCs, increasing their death

We evaluated the ability of immune sera to target CSCs, responsible for metastatic spreading. Cells derived from TUBO and SKBR3 CSC-enriched tumorspheres (23) were incubated with the sera. Sera from control mice did not alter second-generation tumorsphere formation, which was decreased by sera from HER2-vaccinated mice. A greater impairment of tumorsphere generation was induced by sera from xCT-vaccinated mice and, even more, from mice vaccinated with HER2 + xCT (**Fig. 7A–C**). This effect was specifically mediated by vaccine-induced HER2 and, to a greater extent, xCT antibodies, because sera in which these antibodies were depleted by preadsorption on HER2 or xCT recombinant proteins were not able to hinder TUBO tumorsphere generation, whereas preadsorption on the unrelated protein AMOT did not affect sera activity (Supplementary Fig. S6). The decreased CSC self-renewal potential in cells treated with sera from HER2 + xCT- and xCT-vaccinated mice was accompanied by a reduction in cells expressing the TUBO CSC marker $Sca1^+$ (ref. 32; **Fig. 7D**; Supplementary Fig. S7A). Similarly, in SKBR3 tumorspheres, sera from immunized mice significantly reduced the ratio between the percentage of $CD44^+$ and $CD24^+$ cells (**Fig. 7E**; Supplementary Fig. S7A), which correlates with their stemness (33). Because xCT is essential for CSC redox balance (9), intracellular ROS content was evaluated. Whereas ROS content of either TUBO or SKBR3 tumorspheres was not altered by control or HER2-vaccinated mice sera, ROSs were significantly increased in tumorspheres treated with sera from mice vaccinated with HER2 + xCT or xCT (**Fig. 7F** and **G**; Supplementary Fig. S7B). These sera induced apoptosis in CSCs from both cell lines, whereas sera from control or HER2-immunized mice had no effect (**Fig. 7H** and **I**; Supplementary Fig. S7C). Sera from HER2 + xCT- or xCT-vaccinated mice induced ferroptosis in both TUBO and SKBR3 CSCs, as demonstrated by the ability of the iron chelator, DFO, of rescuing cells from their cytotoxic effect, whereas sera from control or HER2-vaccinated mice did not induce cell death either in the absence or presence of DFO (**Fig. 7J** and **K**). Overall, these data demonstrated that anti-xCT vaccination was more effective than

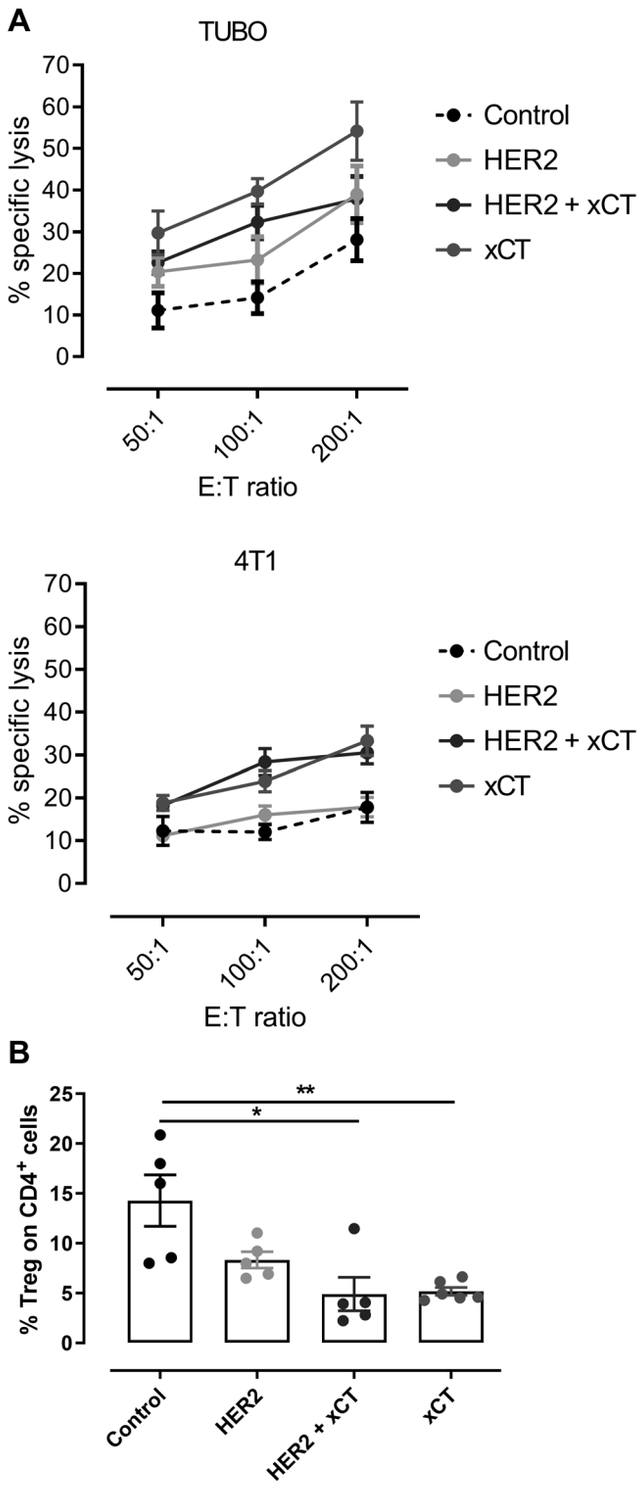

TUBO 50:1	HER2	HER2 + xCT	xCT
Control	ns	ns	$P < 0.05$
HER2	–	ns	$P < 0.05$
HER2 + xCT		–	ns

TUBO 100:1	HER2	HER2 + xCT	xCT
Control	ns	$P < 0.05$	$P < 0.01$
HER2	–	ns	$P < 0.01$
HER2 + xCT		–	ns

TUBO 200:1	HER2	HER2 + xCT	xCT
Control	ns	ns	$P < 0.05$
HER2	–	ns	$P < 0.05$
HER2 + xCT		–	ns

4T1 50:1	HER2	HER2 + xCT	xCT
Control	ns	ns	ns
HER2	–	ns	ns
HER2 + xCT		–	ns

4T1 100:1	HER2	HER2 + xCT	xCT
Control	ns	$P < 0.01$	$P < 0.01$
HER2	–	$P < 0.01$	$P < 0.01$
HER2 + xCT		–	ns

4T1 200:1	HER2	HER2 + xCT	xCT
Control	ns	$P < 0.05$	$P < 0.01$
HER2	–	ns	$P < 0.01$
HER2 + xCT		–	ns

Figure 4.

Anti-xCT vaccination induced T-cell cytotoxicity of xCT$^+$ breast cancer cells and decreased Tregs. **A,** FACS of the percentage of 7-AAD$^+$ dead cells among CFSE$^+$ TUBO or 4T1 cells cocultured for 48 hours with splenocytes from control or vaccinated mice ($N = 4$ per group) at 200, 100, or 50:1 E:T ratios. Graphs show means ± SEM of the percentages of specific lysis. Tables show the results of Student t test analysis (ns, not significant). **B,** Means ± SEM of the percentage of Treg among CD4$^+$ T lymphocytes in peripheral blood of mice at sacrifice ($N \geq 5$ mice per group). Each dot represents a mouse. *, $P < 0.05$; **, $P < 0.01$, Student t test.

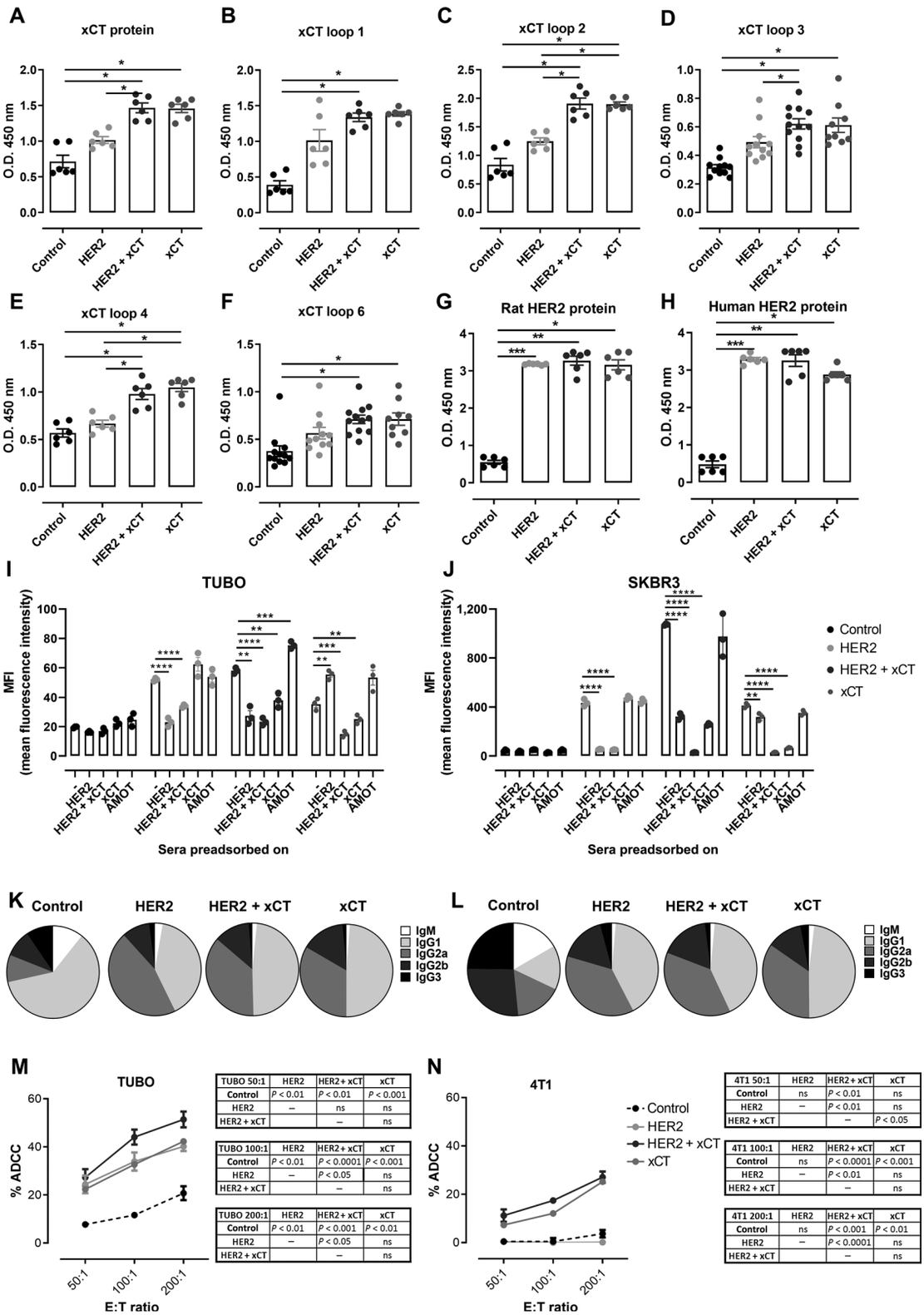

TUBO 50:1	HER2	HER2+xCT	xCT
Control	$P < 0.01$	$P < 0.01$	$P < 0.001$
HER2	–	ns	ns
HER2 + xCT		–	ns

TUBO 100:1	HER2	HER2+xCT	xCT
Control	$P < 0.01$	$P < 0.0001$	$P < 0.001$
HER2	–	$P < 0.05$	ns
HER2 + xCT		–	ns

TUBO 200:1	HER2	HER2+xCT	xCT
Control	$P < 0.01$	$P < 0.001$	$P < 0.01$
HER2	–	$P < 0.05$	ns
HER2 + xCT		–	ns

4T1 50:1	HER2	HER2+xCT	xCT
Control	ns	$P < 0.01$	ns
HER2	–	$P < 0.01$	ns
HER2 + xCT		–	$P < 0.05$

4T1 100:1	HER2	HER2+xCT	xCT
Control	ns	$P < 0.0001$	$P < 0.001$
HER2	–	$P < 0.01$	ns
HER2 + xCT		–	ns

4T1 200:1	HER2	HER2+xCT	xCT
Control	ns	$P < 0.001$	$P < 0.01$
HER2	–	$P < 0.0001$	ns
HER2 + xCT		–	ns

HER2 vaccination in reducing CSCs, making their combination potential for breast cancer treatment.

Discussion

HER2-targeted therapies have significantly improved the outcome of patients with HER2$^+$ breast cancer (34); however, most patients display primary resistance or relapse after treatment, and metastatic breast cancer is considered incurable (34). Therefore, combined therapeutic protocols, which are able to kill the cell populations resistant to HER2 targeting and prevent metastatic spreading, are needed. Therapies able to eradicate CSCs, which are involved in the resistance to most therapies, including HER2-targeted ones (5, 6), may synergize with HER2-directed drugs.

To this end, we developed a combined vaccination approach targeting both HER2 and the CSC-associated antigen xCT, using BoHV-4–based vectors. We tested this immunotherapy in BALB-neuT mice, an ideal model whose tumors display a high homology to human HER2$^+$ breast cancer (18) and contain early disseminating cancer cells (eDCC) that move to the bone marrow, and hence to lungs where they give rise to metastasis (35, 36).

HER2 and xCT represent self-antigens in BALB-neuT mice. To break immune tolerance to rat HER2, we used a BoHV-4–based vector coding for a chimeric rat/human HER2. This vaccine was designed to be suitable for both BALB-neuT mice and humans, thanks to the ability of xenogeneic sequences to break immune tolerance to self-antigens. Indeed, the chimeric vaccine induces a superior immune response than rat HER2 vaccines in BALB-neuT mice (21). BoHV-4–based vaccination induced a strong and specific immune response to both HER2 and xCT. HER2 vaccination induced a humoral response, and the activation of NK and Th cells in both primary tumors and lung metastases, but not of lung-infiltrating CD8$^+$ T lymphocytes. On the contrary, anti-xCT vaccination induced both a polyclonal antibody response and the activation of tumor- and lung-infiltrating NK, CD4$^+$, and CD8$^+$ T cells. The lack of HER2-directed cytotoxicity is likely due to the thymic deletion of high avidity HER2-specific CD8$^+$ T cells in BALB-neuT mice (31), where a CD4$^+$ T-cell repertoire escapes central tolerance (31); this allows for the induction of an HER2 antibody response necessary for protection from tumor development (18, 19, 37). Anti-xCT vaccination, instead, breaks immune tolerance and induces a T cytotoxic response, which exerts a key role in transplantable models of mammary cancer (16). Whereas naïve T lymphocytes lack xCT and rely on the uptake of cysteine released from antigen-presenting cells for the synthesis of GSH, xCT expression is induced on T lymphocytes upon activation and is necessary for their proliferation *in vitro* (38). However, *in vivo* compensative mechanisms make xCT dispensable for T-cell proliferation and antitumor responses (39). Of note, the induction of xCT-specific cytotoxic T cells is exclusive of BoHV-4–based vaccines, because neither DNA nor virus-like particle (VLP)–based xCT vaccines activate them (8, 17), indicating that BoHV-4 is superior in breaking immune tolerance to xCT. This is likely due to viral vectors' intrinsic immunogenicity, which creates an inflammatory environment that potentiates T lymphocyte activation (40). In addition, xCT vaccination decreased Tregs, likely through the reduction in glutamate export from xCT$^+$ cells, thus preventing the proliferative effect exerted by metabotropic glutamate receptor 1 on Tregs (10). Further studies are needed to evaluate possible direct effects of xCT targeting on Tregs.

HER2 and xCT vaccination induced a strong antibody response. Anti-xCT vaccination induced epitope spreading, with the production of antibodies able to recognize HER2. A similar phenomenon was observed using a DNA vaccine coding for the extracellular and transmembrane domain of rat HER2, which induced a spread of the immune response to HER2 intracellular epitopes (31) and antibodies able to recognize human HER2 (37). Vaccine-induced antibodies exerted both direct and indirect effects on cancer cells, inducing ADCC and directly affecting their viability. Of note, SKBR3 cells were more sensitive than TUBO cells. Because sera from HER2-vaccinated mice bind with similar efficacy rat and human HER2, it is improbable that the greater sensitivity of SKBR3 was caused by a higher induction of human than rat antibodies by the chimeric vaccine. Instead, SKBR3 may be more sensitive than TUBO cells by virtue of their higher expression of both HER2 and xCT. Indeed, SKBR3 bears *HER2* gene amplification, resulting in a highly active HER2 signaling that promotes cell survival and proliferation (41). The higher expression of HER2 and xCT allowed a higher recognition of SKBR3 than TUBO cells by immune sera, which resulted in a higher inhibition of their viability. The induction of an antibody response was particularly important for the elimination of CSCs, which downregulate MHC class I becoming less sensitive to T-cell killing (32). Indeed, sera from vaccinated mice, and in particular from mice vaccinated with xCT alone or combined with HER2, strongly inhibited CSC self-renewal and altered their redox balance, inducing ROS accumulation and ferroptosis.

Metastatic dissemination often occurs during the early phases of cancer progression, when the frequency of CSCs in primary lesions is higher than in more advanced tumors (35). In *Her2* transgenic mice, 80% of metastases derive from eDCCs, which display moderate HER2 expression. eDCCs possess CSC features, such as Wnt pathway activation, and inhibition of p38, E-cadherin– and β-catenin–mediated junction formation, allowing for an epithelial-to-mesenchymal transition–like invasive program (35, 42). Of note, by decreasing intracellular ROS, xCT inhibits p38, thus diminishing caveolin-1 and the recruitment of β-catenin to the plasma membrane, suggesting that xCT may contribute to the invasiveness of eDCCs (43). On the contrary, HER2 expression is low in early lesions and in eDCCs, whereas it increases during cancer growth, and HER2 activation is more involved in the proliferation of disseminated cells than in their migration (35). Despite HER2 promoting breast CSC self-renewal (44), HER2 inhibition leads to Notch1 activation, thus promoting CSC expansion, tumor recurrence, and metastasis (45, 46). CSCs from SKBR3 cells are resistant to HER2-targeted therapies (41), in accordance with our data showing that antibodies from HER2-vaccinated mice exerted a mild inhibitory effect on SKBR3 tumorspheres, which are killed by xCT antibodies. Overall, our data and the

Figure 5.

Vaccination induced specific antibodies that mediated ADCC. ELISA of pooled sera from control or vaccinated mice on mouse xCT protein (**A**); peptides representing xCT extracellular loops 1 (**B**), 2 (**C**), 3 (**D**), 4 (**E**), or 6 (**F**); and extracellular domains of rat (**G**) or human HER2 (**H**). Graphs show means ± SEM of two pools analyzed in three independent experiments. FACS mean fluorescence intensity (MFI) of TUBO (**I**) and SKBR3 (**J**) cells stained with pooled sera, unprocessed (−) or preadsorbed on HER2, xCT, HER2 and xCT, or AMOT proteins ($N = 3$). *, $P < 0.05$; **, $P < 0.01$; ***, $P < 0.001$; ****, $P < 0.0001$, Student t test. Proportion of anti-xCT (**K**) and anti-HER2 Ig (**L**) isotypes in the sera of mice (ELISA). Mean ± SEM of the percentage of ADCC of CFSE$^+$ TUBO (**M**) or 4T1 (**N**) cells incubated with sera (1:50) pooled from control or vaccinated mice and splenocytes from naïve mice at 200, 100, and 50:1 E:T ratios. Tables show the results of Student t test analysis (ns, not significant).

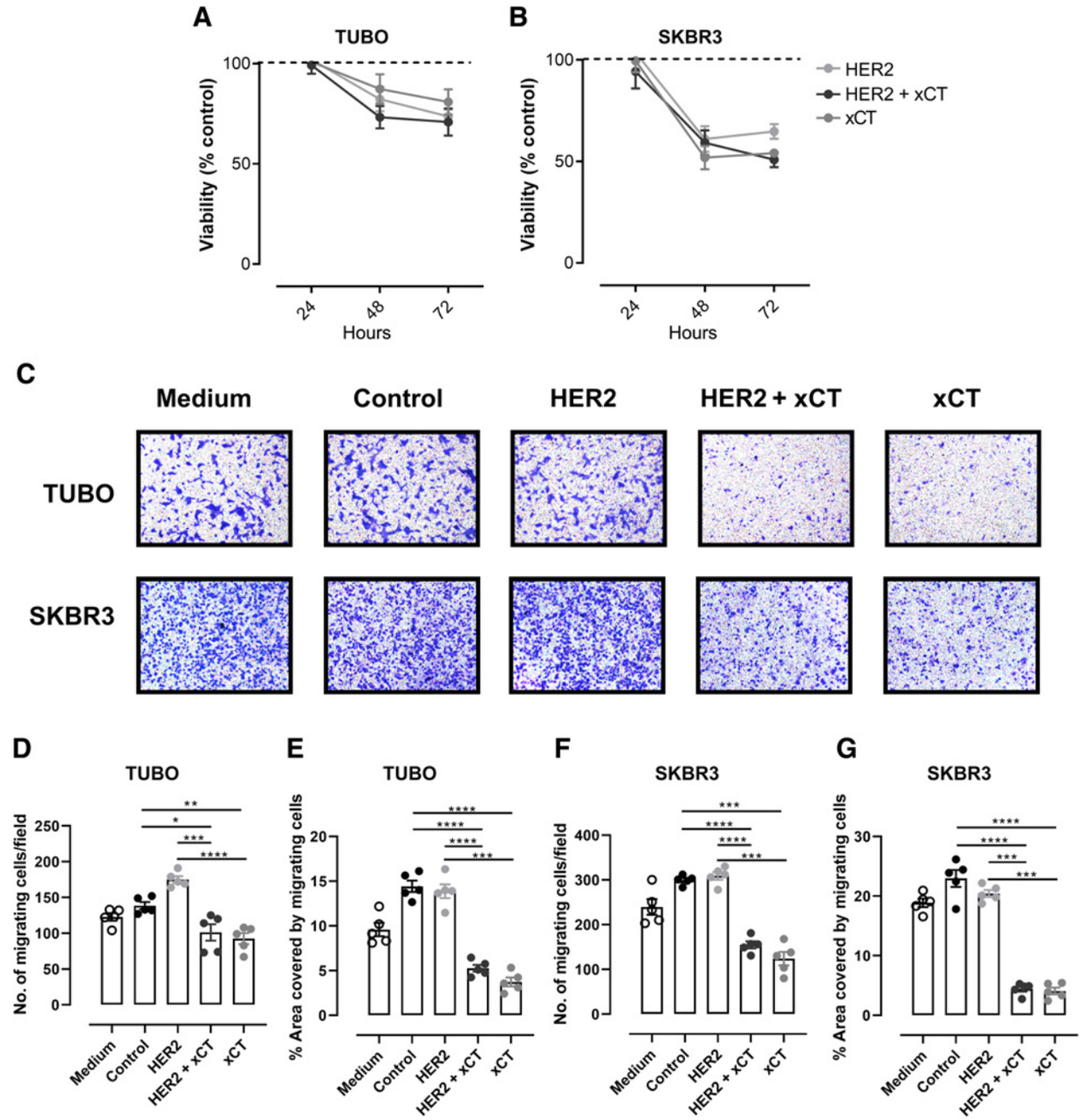

Figure 6.

HER2 and xCT antibodies differentially impaired cell viability and migration. Means ± SEM of the percentage of cell viability of TUBO (**A**) and SKBR3 (**B**) cells incubated with sera (1:50) pooled from vaccinated mice compared with control sera. **C–G,** Transwell migration assay of TUBO and SKBR3 cells incubated with the sera. **C,** Representative images of crystal violet–stained migrated cells. Graphs show means ± SEM of the number of migrated cells (**D** and **F**) and the percentage of area covered by migrated cells (**E** and **G**) in five different fields. *, $P < 0.05$; **, $P < 0.01$; ***, $P < 0.001$; ****, $P < 0.0001$, Student *t* tests. Results from three independent experiments.

literature suggest that HER2 and xCT vaccination may act synergistically, with anti-HER2 immune response mainly affecting cancer growth, and anti-xCT hindering metastatic spreading.

xCT is expressed on astrocytes, some myeloid cells, and activated T cells (9). However, the safety of xCT targeting is supported by the lack of detrimental organ alterations and developmental and immunologic defects in xCT-knockout mice (39, 47) and in Subtle gray mice harboring a spontaneous protein-null xCT mutation (48). The xCT inhibitor sulfasalazine is widely used for the treatment of inflammatory diseases such as Crohn disease and ulcerative colitis (49). No adverse events were observed in xCT-vaccinated mice (8, 16), and no alterations or immune infiltration were observed in the central nervous

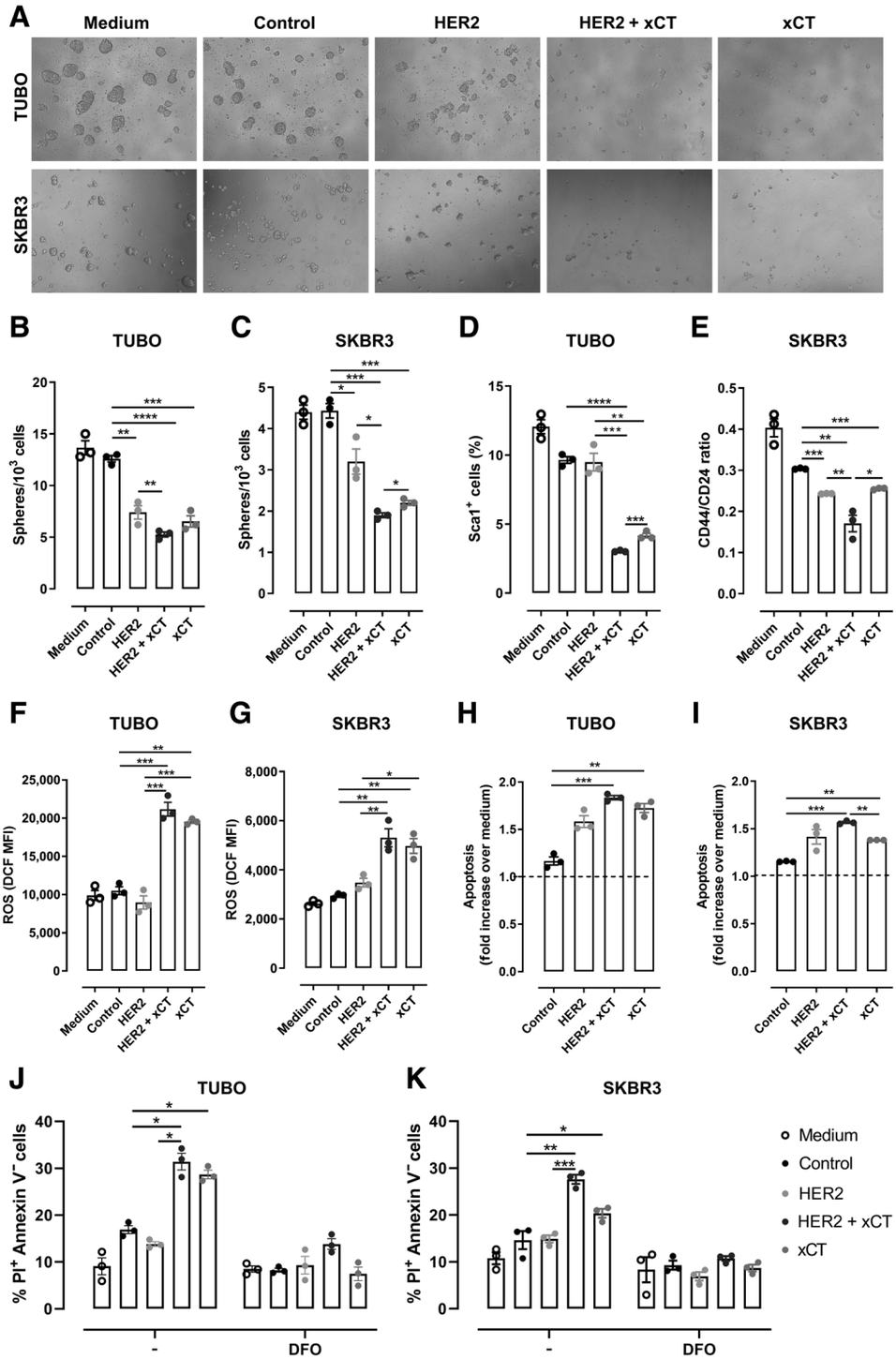

Figure 7.

xCT antibodies induced CSC cell death. **A–I,** Dissociated TUBO- or SKBR3-derived tumorspheres were incubated for 5 days with or without sera (1:50) from vaccinated mice. **A,** Representative ($N = 3$) images of tumorspheres (magnification, 10×). **B** and **C,** Sphere-generating ability (number of tumorspheres generated every 10^3 plated cells). Means ± SEM of the percentage of $Sca1^+$ cells in TUBO (**D**) or of the ratio between $CD44^+$ and $CD24^+$ cells in SKBR3 (**E**) tumorspheres. **F** and **G,** FACS of intracellular ROS [means ± SEM of 2′,7′-dichlorofluorescein (DCF) mean fluorescence intensity (MFI)]. **H** and **I,** Apoptosis, reported as mean ± SEM of the fold increase of Annexin V^+ cells compared with tumorspheres cultured without sera. **J** and **K,** Ferroptosis of TUBO or SKBR3 tumorspheres incubated for 24 hours with or without sera (1:50) ± DFO (50 μmol/L). Means ± SEM of the percentage of Annexin V^-/propidium iodide $(PI)^+$ cells. Results from three independent experiments. *, $P < 0.05$; **, $P < 0.01$; ***, $P < 0.001$; ****, $P < 0.0001$, Student t test.

system of mice vaccinated with xCT-targeting VLPs (17). Vaccination against xCT does not compromise the immune response. xCT vaccination induced a specific cytotoxic T-cell response, confirming that T lymphocytes *in vivo* do not depend on xCT (39), and suggesting that they were not targeted by anti-xCT immune responses. Similarly, Th and B lymphocytes were not affected by anti-xCT vaccination, because similar amounts of HER2 antibodies were observed in mice vaccinated with HER2 alone or combined with xCT. Therefore, the possibility of targeting xCT for cancer treatment has attracted the attention of pharmaceutical companies (39).

The clinical successes of checkpoint inhibitors and of chimeric antigen receptor T cells has opened a new golden age for cancer immunotherapy, leading many researchers to focus on these new immunotherapies. However, we believe that vaccination still represents a promising approach for cancer treatment. Vaccination is a cost-effective strategy as compared with mAbs and lymphocyte adoptive therapies (7). Breast cancer incidence is increasing in low-income countries, where the lack of resources makes it a neglected disease, causing high mortality rates and health inequity (2). The development of effective anti-HER2 vaccines might provide more accessible therapies that are able to improve life expectancy of hundreds of thousands of women who currently have to face disability and premature death. In this view, BoHV-4 represents a promising vector because of its absence of pathogenicity or oncogenic activity, the possibility of performing repeated boosts without inducing virus-neutralizing antibodies, and its ability to induce strong immune responses breaking tolerance to cancer-associated antigens (50).

Our findings demonstrated that xCT vaccination synergized with HER2-directed immunotherapy to limit breast cancer progression. Whereas HER2 vaccination mainly impairs the growth of primary tumor, anti-xCT vaccination strongly affects CSCs and decreases metastases. This immunotherapeutic approach could be further combined with treatments such as immune checkpoint inhibitors or chemotherapy to induce anticancer immune responses, providing new options in the management of $HER2^{+}$ breast cancer.

Disclosure of Potential Conflicts of Interest

L. Conti reports grants from Fondazione AIRC per la Ricerca sul cancro and nonfinancial support from Fondazione Ricerca Molinette during the conduct of the study. R. Ruiu reports other from Italian Foundation/Association for Cancer Research (FIRC-AIRC; fellowship) during the conduct of the study. E. Quaglino reports grants from Fondazione AIRC per la Ricerca sul cancro and nonfinancial support from Fondazione Ricerca Molinette during the conduct of the study. F. Cavallo reports grants from Fondazione AIRC per la Ricerca sul cancro and nonfinancial support from Fondazione Ricerca Molinette during the conduct of the study. No potential conflicts of interest were disclosed by the other authors.

Authors' Contributions

L. Conti: Conceptualization, data curation, formal analysis, supervision, investigation, methodology, writing–original draft, writing–review and editing. **E. Bolli:** Investigation, writing–review and editing. **A. Di Lorenzo:** Investigation. **V. Franceschi:** Investigation. **F. Macchi:** Investigation. **F. Riccardo:** Investigation, writing–review and editing. **R. Ruiu:** Investigation, writing–review and editing. **L. Russo:** Investigation. **E. Quaglino:** Conceptualization, writing–review and editing. **G. Donofrio:** Conceptualization, resources, supervision, writing–review and editing. **F. Cavallo:** Conceptualization, resources, data curation, supervision, funding acquisition, writing–original draft, project administration, writing–review and editing.

Acknowledgments

The research leading to these results has received funding from AIRC under IG 2018 - ID. 21468 project – principal investigator F. Cavallo, from Fondazione Ricerca Molinette Onlus, and from the University of Torino (Torino, Italy). R. Ruiu was supported by an FIRC-AIRC fellowship for Italy during the conduct of the study. The authors thank Dr. Irene Fiore Merighi for breeding and genotyping the mice.

The costs of publication of this article were defrayed in part by the payment of page charges. This article must therefore be hereby marked *advertisement* in accordance with 18 U.S.C. Section 1734 solely to indicate this fact.

Received January 28, 2020; revised April 16, 2020; accepted June 3, 2020; published first June 12, 2020.

References

1. Bray F, Ferlay J, Soerjomataram I, Siegel RL, Torre LA, Jemal A. Global cancer statistics 2018: GLOBOCAN estimates of incidence and mortality worldwide for 36 cancers in 185 countries. CA Cancer J Clin 2018;68:394–424.
2. Ginsburg O, Bray F, Coleman MP, Vanderpuye V, Eniu A, Kotha SR, et al. The global burden of women's cancers: a grand challenge in global health. Lancet 2017;389:847–60.
3. Wang J, Xu B. Targeted therapeutic options and future perspectives for HER2-positive breast cancer. Signal Transduct Target Ther 2019;4:34.
4. Krasniqi E, Barchiesi G, Pizzuti L, Mazzotta M, Venuti A, Maugeri-Sacca M, et al. Immunotherapy in HER2-positive breast cancer: state of the art and future perspectives. J Hematol Oncol 2019;12:111.
5. Seo AN, Lee HJ, Kim EJ, Jang MH, Kim YJ, Kim JH, et al. Expression of breast cancer stem cell markers as predictors of prognosis and response to trastuzumab in HER2-positive breast cancer. Br J Cancer 2016;114:1109–16.
6. Ruiu R, Tarone L, Rolih V, Barutello G, Bolli E, Riccardo F, et al. Cancer stem cell immunology and immunotherapy: Harnessing the immune system against cancer's source. Prog Mol Biol Transl Sci 2019;164:119–88.
7. Quaglino E, Conti L, Cavallo F. Breast cancer stem cell antigens as targets for immunotherapy. Semin Immunol 2020;47:101386.
8. Lanzardo S, Conti L, Rooke R, Ruiu R, Accart N, Bolli E, et al. Immunotargeting of antigen xCT attenuates stem-like cell behavior and metastatic progression in breast cancer. Cancer Res 2016;76:62–72.
9. Ruiu R, Rolih V, Bolli E, Barutello G, Riccardo F, Quaglino E, et al. Fighting breast cancer stem cells through the immune-targeting of the xCT cystine-glutamate antiporter. Cancer Immunol Immunother 2018;68:131–41.
10. Long Y, Tao H, Karachi A, Grippin AJ, Jin L, Chang YE, et al. Dysregulation of glutamate transport enhances Treg function that promotes VEGF blockade resistance in glioblastoma. Cancer Res 2020;80:499–509.
11. Dornier E, Rabas N, Mitchell L, Novo D, Dhayade S, Marco S, et al. Glutaminolysis drives membrane trafficking to promote invasiveness of breast cancer cells. Nat Commun 2017;8:2255.
12. Briggs KJ, Koivunen P, Cao S, Backus KM, Olenchock BA, Patel H, et al. Paracrine induction of HIF by glutamate in breast cancer: EglN1 senses cysteine. Cell 2016;166:126–39.
13. Dixon SJ, Patel DN, Welsch M, Skouta R, Lee ED, Hayano M, et al. Pharmacological inhibition of cystine-glutamate exchange induces endoplasmic reticulum stress and ferroptosis. Elife 2014;3:e02523.
14. Linares V, Alonso V, Domingo JL. Oxidative stress as a mechanism underlying sulfasalazine-induced toxicity. Expert Opin Drug Saf 2011;10:253–63.
15. Robe PA, Martin DH, Nguyen-Khac MT, Artesi M, Deprez M, Albert A, et al. Early termination of ISRCTN45828668, a phase 1/2 prospective, randomized study of sulfasalazine for the treatment of progressing malignant gliomas in adults. BMC Cancer 2009;9:372.
16. Donofrio G, Tebaldi G, Lanzardo S, Ruiu R, Bolli E, Ballatore A, et al. Bovine herpesvirus 4-based vector delivering the full length xCT DNA efficiently protects mice from mammary cancer metastases by targeting cancer stem cells. Oncoimmunology 2018;7:e1494108.

17. Bolli E, O'Rourke JP, Conti L, Lanzardo S, Rolih V, Christen JM, et al. A virus-like-particle immunotherapy targeting epitope-specific anti-xCT expressed on cancer stem cell inhibits the progression of metastatic cancer in vivo. Oncoimmunology 2017;7:e1408746.
18. Conti L, Ruiu R, Barutello G, Macagno M, Bandini S, Cavallo F, et al. Microenvironment, oncoantigens, and antitumor vaccination: lessons learned from BALB-neuT mice. Biomed Res Int 2014;2014:534969.
19. Jacca S, Rolih V, Quaglino E, Franceschi V, Tebaldi G, Bolli E, et al. Bovine herpesvirus 4-based vector delivering a hybrid rat/human HER-2 oncoantigen efficiently protects mice from autochthonous Her-2(+) mammary cancer. Oncoimmunology 2016;5:e1082705.
20. Rovero S, Amici A, Di Carlo E, Bei R, Nanni P, Quaglino E, et al. DNA vaccination against rat her-2/Neu p185 more effectively inhibits carcinogenesis than transplantable carcinomas in transgenic BALB/c mice. J Immunol 2000; 165:5133–42.
21. Quaglino E, Mastini C, Amici A, Marchini C, Iezzi M, Lanzardo S, et al. A better immune reaction to Erbb-2 tumors is elicited in mice by DNA vaccines encoding rat/human chimeric proteins. Cancer Res 2010;70:2604–12.
22. Geninatti Crich S, Cadenazzi M, Lanzardo S, Conti L, Ruiu R, Alberti D, et al. Targeting ferritin receptors for the selective delivery of imaging and therapeutic agents to breast cancer cells. Nanoscale 2015;7:6527–33.
23. Conti L, Lanzardo S, Arigoni M, Antonazzo R, Radaelli E, Cantarella D, et al. The noninflammatory role of high mobility group box 1/Toll-like receptor 2 axis in the self-renewal of mammary cancer stem cells. FASEB J 2013;27: 4731–44.
24. Donofrio G, Herath S, Sartori C, Cavirani S, Flammini CF, Sheldon IM. Bovine herpesvirus 4 is tropic for bovine endometrial cells and modulates endocrine function. Reproduction 2007;134:183–97.
25. Regis G, Icardi L, Conti L, Chiarle R, Piva R, Giovarelli M, et al. IL-6, but not IFN-gamma, triggers apoptosis and inhibits *in vivo* growth of human malignant T cells on STAT3 silencing. Leukemia 2009;23:2102–8.
26. Bandini S, Macagno M, Hysi A, Lanzardo S, Conti L, Bello A, et al. The non-inflammatory role of C1q during Her2/neu-driven mammary carcinogenesis. Oncoimmunology 2016;5:e1253653.
27. Macagno M, Bandini S, Stramucci L, Quaglino E, Conti L, Balmas E, et al. Multiple roles of perforin in hampering ERBB-2 (Her-2/neu) carcinogenesis in transgenic male mice. J Immunol 2014;192:5434–41.
28. Győrffy B, Lanczky A, Eklund AC, Denkert C, Budczies J, Li Q, et al. An online survival analysis tool to rapidly assess the effect of 22,277 genes on breast cancer prognosis using microarray data of 1,809 patients. Breast Cancer Res Treat 2010; 123:725–31.
29. Harris IS, Treloar AE, Inoue S, Sasaki M, Gorrini C, Lee KC, et al. Glutathione and thioredoxin antioxidant pathways synergize to drive cancer initiation and progression. Cancer Cell 2015;27:211–22.
30. Liu S, Cong Y, Wang D, Sun Y, Deng L, Liu Y, et al. Breast cancer stem cells transition between epithelial and mesenchymal states reflective of their normal counterparts. Stem Cell Reports 2014;2:78–91.
31. Rolla S, Nicolo C, Malinarich S, Orsini M, Forni G, Cavallo F, et al. Distinct and non-overlapping T cell receptor repertoires expanded by DNA vaccination in wild-type and HER-2 transgenic BALB/c mice. J Immunol 2006;177:7626–33.
32. Tallerico R, Conti L, Lanzardo S, Sottile R, Wagner AK, Johansson MH, et al. NK cells control breast cancer and related cancer stem cell hematological spread. Oncoimmunology 2017;6:1–11.
33. Li W, Ma H, Zhang J, Zhu L, Wang C, Yang Y. Unraveling the roles of CD44/CD24 and ALDH1 as cancer stem cell markers in tumorigenesis and metastasis. Sci Rep 2017;7:13856.
34. Harbeck N, Gnant M. Breast cancer. Lancet 2017;389:1134–50.
35. Hosseini H, Obradovic MM, Hoffmann M, Harper KL, Sosa MS, Werner-Klein M, et al. Early dissemination seeds metastasis in breast cancer. Nature 2016;540: 552–8.
36. Husemann Y, Geigl JB, Schubert F, Musiani P, Meyer M, Burghart E, et al. Systemic spread is an early step in breast cancer. Cancer Cell 2008; 13:58–68.
37. Quaglino E, Riccardo F, Macagno M, Bandini S, Cojoca R, Ercole E, et al. Chimeric DNA vaccines against ErbB2+ carcinomas: from mice to humans. Cancers 2011;3:3225–41.
38. Garg SK, Yan Z, Vitvitsky V, Banerjee R. Differential dependence on cysteine from transsulfuration versus transport during T cell activation. Antioxid Redox Signal 2011;15:39–47.
39. Arensman MD, Yang XS, Leahy DM, Toral-Barza L, Mileski M, Rosfjord EC, et al. Cystine-glutamate antiporter xCT deficiency suppresses tumor growth while preserving antitumor immunity. Proc Natl Acad Sci U S A 2019;116: 9533–42.
40. Larocca C, Schlom J. Viral vector-based therapeutic cancer vaccines. Cancer J 2011;17:359–71.
41. Weigelt B, Lo AT, Park CC, Gray JW, Bissell MJ. HER2 signaling pathway activation and response of breast cancer cells to HER2-targeting agents is dependent strongly on the 3D microenvironment. Breast Cancer Res Treat 2010;122:35–43.
42. Harper KL, Sosa MS, Entenberg D, Hosseini H, Cheung JF, Nobre R, et al. Mechanism of early dissemination and metastasis in Her2(+) mammary cancer. Nature 2016;540:588–92.
43. Chen RS, Song YM, Zhou ZY, Tong T, Li Y, Fu M, et al. Disruption of xCT inhibits cancer cell metastasis via the caveolin-1/beta-catenin pathway. Oncogene 2009;28:599–609.
44. Korkaya H, Wicha MS. HER2 and breast cancer stem cells: more than meets the eye. Cancer Res 2013;73:3489–93.
45. Abravanel DL, Belka GK, Pan TC, Pant DK, Collins MA, Sterner CJ, et al. Notch promotes recurrence of dormant tumor cells following HER2/neu-targeted therapy. J Clin Invest 2015;125:2484–96.
46. Osipo C, Patel P, Rizzo P, Clementz AG, Hao L, Golde TE, et al. ErbB-2 inhibition activates Notch-1 and sensitizes breast cancer cells to a gamma-secretase inhibitor. Oncogene 2008;27:5019–32.
47. Sato H, Shiiya A, Kimata M, Maebara K, Tamba M, Sakakura Y, et al. Redox imbalance in cystine/glutamate transporter-deficient mice. J Biol Chem 2005; 280:37423–9.
48. Chintala S, Li W, Lamoreux ML, Ito S, Wakamatsu K, Sviderskaya EV, et al. Slc7a11 gene controls production of pheomelanin pigment and proliferation of cultured cells. Proc Natl Acad Sci U S A 2005;102: 10964–9.
49. Damiao A, de Azevedo MFC, Carlos AS, Wada MY, Silva TVM, Feitosa FC. Conventional therapy for moderate to severe inflammatory bowel disease: a systematic literature review. World J Gastroenterol 2019;25: 1142–57.
50. Donofrio G, Cavirani S, Simone T, van Santen VL. Potential of bovine herpesvirus 4 as a gene delivery vector. J Virol Methods 2002;101:49–61.